Tectonophysics, 22 (1974) 335—353

PALAEOMAGNETIC RESULTS ON A DOLERITIC SILL OF DECCAN TRAP AGE IN THE SONHAT COAL BASIN, INDIA*

C.T. KLOOTWIJK**

Palaeomagnetic Laboratory, State University Utrecht, Utrecht (The Netherlands)

(Accepted for publication January 23, 1974)

ABSTRACT

Klootwijk, C.T., 1974. Palaeomagnetic results on a doleritic sill of Deccan Trap age in the Sonhat Coal Basin, India. Tectonophysics, 22:335—353.

Palaeomagnetic research was carried out on a thick doleritic sill of Late Deccan Trap age (60.0 ± 3.0 m.y.) in the Sonhat Coal Basin, Central India. The samples, 104 in all, showed a magnetization with normal polarity.

The characteristic mean-site direction for this sill, obtained after treatment in alternating fields and by thermal methods, becomes coincident with the mean Upper Deccan Trap direction of the Western Ghats, after application of a correction for the slight dip of the adjacent strata. This indicates that the tectonic disturbances are of post-intrusional age.

The present results do not support earlier palaeomagnetic arguments in favour of the hypothesis of a prolonged magmatic activity on the Indian subcontinent, lasting from the Rajmahal Trap effusion (100—105 m.y.) till the Deccan Trap effusion (60—65 m.y.).

During thermal treatment of the specimens, evidence for a partial self-reversal of magnetization was found.

INTRODUCTION

During the Mesozoic—Cenozoic northward drift of the Indian subcontinent, two phases of major volcanic activity have occurred. During the oldest phase (100—105 m.y.: McDougall and McElhinny, 1970) the Rajmahal Trap basalts extruded over a rather restricted area in Northeast India. The younger phase (60—65 m.y.: Wellmann and McElhinny, 1970; Kaneoka and Haramura, 1973) resulted in the extrusion of the vast sequence of Deccan Trap basalts over extensive areas in Western and Central India. In the intervening belt of Gondwana basins (Fig. 1) in Sarguja and the Damodar Valley, hypabyssal igneous activity has given rise to doleritic dykes and sills (Fox, 1934). This hypabyssal igneous activity is remarkable with respect to the nearly complete absence of igneous activity in the other Gondwana belts in Eastern and Central India, i.e. the Godavary Valley and the Mahanadi Valley.

---

* This paper forms part of a doctoral thesis.

** At present: Department of Geology and Mineralogy, State University Utrecht.

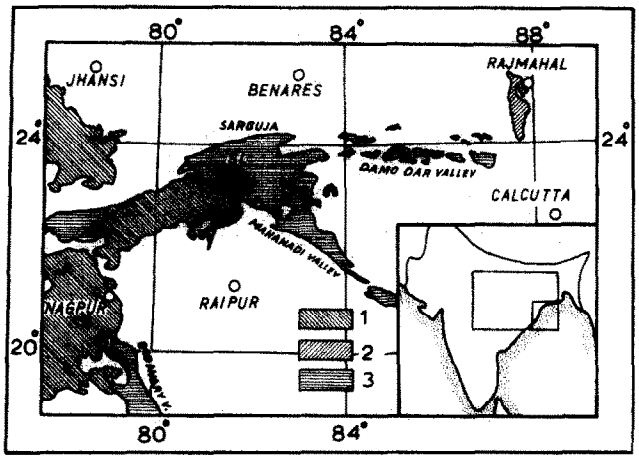

Fig. 1. Geological sketch map of Central Eastern India. *S.L.* = Sampling locality of the sill (Sonhat coalfield). *1* = Deccan Traps, *2* = Rajmahal Traps, *3* = Gondwana outcrops. Unshaded = Basement and Alluvium.

The lava flows from the Rajmahal Trap sequence as well as from the Deccan Trap sequence are of tholeiitic composition, and the rocks bear great resemblance to each other. Therefore, the hypothesis that both extrusions do represent distinct phases of a possible continuous magmatic activity, is frequently referred to in Indian geology (Pascoe, 1959, 1963; Krishnan, 1968). It is thought (Athavale and Verma, 1970) that this igneous activity commenced in Eastern India with the eruption of the Rajmahal Trap lavas and passed subsequently through a hypabyssal phase with dyke and sill intrusions in the intervening tract of Gondwana coal basins, to the eruption of the Deccan Trap lavas in Western India. The generally assumed presence of the oldest Deccan flows in the eastern Deccan Trap area, with the younger flows occurring more to the west (Krishnan, 1968, p. 418) might be interpreted in favour of this hypothesis. However, convincing evidence for this hypthesis of prolonged magmatic activity, which would pass over at least 40 m.y., has not yet been obtained. Radiometric datings on the sills and dykes in the belt of Gondwana basins have not been available up to now. Moreover, the already long existing view of an overall decrease in age of the Deccan Trap flows in western direction seems to be based on rather old stratigraphical fieldwork (Krishnan, 1968, p. 418).

Recent radiometric datings of the Deccan Trap basalts (Wellmann and McElhinny, 1970) do not support such an age decrease in a westerly direction.

Recently, Athavale and Verma (1970) have interpreted their palaeomagnetic results of undated dykes from the Damodar Valley and the Sarguja area in support of this previously postulated continuous magmatic

activity hypothesis. However, their palaeomagnetic data seem ambiguous. Their results were obtained after AF-treatment, generally up to 100 Oe peak value only, and they refrained from applying possible dip corrections to their results.

The present palaeomagnetic results from a large sill, which is exposed in one of the Gondwana basins in the intervening tract (Fig. 1), were obtained after elaborate alternating field- and thermal-cleaning procedures. A newly obtained radiometric dating enables us to settle the question of possible post-intrusional tectonic disturbances. Therefore, it seems worthwhile to compare the present results with those of Athavale and Verma which favour continuous magmatic activity.

GEOLOGICAL SETTING

The small Sonhat coalfield (about 800 km^2) forms part of the large continuous track of Gondwana exposures in Central India (Fig. 1). This track continues to the east into the Damodar Valley as a series of separate outcrops.

The Gondwana strata (Table I) have a main northward dip. In the southern part of the Sonhat basin a large expanse of Talchir rocks is exposed. To the north these Talchir outcrops are followed in turn by the overlying Mahadeva beds which occupy a very large area to the north.

Restricted in general to the Barakar beds, a large sill is intruded. This sill can be traced continuously over a distance of at least 60 km as a ENE—WSW stretching escarpment ("ghat") and continues probably into the Sohagpur basin to the west and the Jhilmili basin to the east (Fermor, 1914).

During a survey study of the Sonhat coalfield, Fermor (1914) observed almost everywhere along the "ghat" a marked northern dip of the strata, ranging between 6 and 20 degrees and averaging about 10—12 degrees. According to drilling data (D. Mukherjee and P.K. Dutta, personal communication, 1969), the sill reaches a thickness of 130 m in the sampling area and dips about 10—15 degrees in NNW direction.

TABLE I

Geological formations in the Sonhat basin

	Deccan Traps, including dykes and sills
Upper Gondwanas	Mahadevas
Lower Gondwanas	{ Barakars Talchirs
	Archaeans

The central part of this sill is a very coarsely crystalline dolerite, becoming finer textured in its upper and lower portion, with the actual margins being basaltic for about one meter. The characteristic minerals of this doleritic sill are basic plagioclase, titano-augite, rather iron-rich olivine and Fe—Ti-oxides, frequently with interstitial patches of partly devitrified and altered glass. Olivine is more abundant in the more peripheral portions of the sill than in the coarsely crystalline centre. The prevailing ore-minerals are generally idiomorph crystals of ilmenite and magnetite, the latter with well developped ilmenite lamellae and patches and to a minor extent secondary haematite. Accessory small crystals of chalcopyrite and bornite are present. In specimens from several sites the ore-minerals showed signs of limonitisation, and in some sites the olivine has partially been decomposed to serpentine with formation of secondary iron-hydroxides.

From the local geology of the Sonhat basin, no definite evidence concerning the age of this sill can be deduced. Neither the sill, nor the accompanying dykes are found to traverse the Mahadeva beds (D. Mukherjee, personal communication, 1969), which predate both the Rajmahal Trap- and the Deccan Trap-eruption phase. However, the vicinity of the Deccan Trap outliers of comparable composition, strongly favours a Deccan Trap age for this sill (Fermor, 1914; Fox, 1934; Wadia, 1953; Pascoe 1963; Krishnan, 1968). In order to determine the age of this sill, some samples for a K/Ar dating were obtained from a fresh drill core.

The geological setting of the basin gives no definite evidence as to whether the northward dip of the sill results from an intrusion aligned parallel to the already dipping Gondwana strata, or whether the dip of this sill is due to post-intrusional tectonic disturbances. This question will be discussed in the next sections on the basis of combined radiometric and palaeomagnetic results.

SAMPLING DETAILS

Core-samples, 104 in all, of 2.5 cm diameter were obtained by means of a portable drill. Orientation was performed by a normal compass and a clinometer. The distance from the rocks to the compass was at least 20 cm. As the mean intensity of the NRM is about $3 \cdot 10^{-3}$ emu/cm^3, it may be safely assumed that orientation error, due to to the rocks' own magnetization, has been avoided.

At least eight samples were drilled at each site. Two sections were sampled on the ENE—WSW stretching escarpment ("ghat") formed by the sill outcrop. On the most eastern section along the Baikunthapur—Sonhat road, nine sites were sampled through eastern section along the Baikunthapur—Sonhat road, nine sites were sampled through the lower half of the 130 m thick sill, i.e. from about 70 m (ISNI) above the base of the sill to about 30 m (ISNA) above the base. Some of the exposures along this road showed signs of weathering, but all samples were drilled from the most fresh parts. At the second section in the Jhumka Nala, several kilometers further to the west,

four more sites (ISOA—ISOD) covering the upper 20 m of the sill were sampled in very fresh stream-bed exposures.

RESULTS

The NRM and induced magnetization of 185 specimens (2.2 cm height and 2.5 cm diameter) was measured with an astatic magnetometer (Table II). The initial measurements reveal magnetization directions of normal polarity which group well in the NW-quadrant, mostly with shallow upward inclinations (Fig. 2A, 3A1, 3A2, 4). The specimens from the road section (sites ISNA—ISNI) show a more pronounced streaking towards the present local field direction, dipping about 30 degrees downwards. Initial NRM intensities ranged from 1 to $9 \cdot 10^{-3}$ emu/cm^3 in both sections, with a mean range of 2—$3 \cdot 10^{-3}$ emu/cm^3 in specimens from the road section (ISNA—ISNI) and 3—$4 \cdot 10^{-3}$ emu/cm^3 in specimens from the Jhumka Nala section (ISOA—ISOD). The intensity of induced magnetization showed a mean range of 1—$2 \cdot 10^{-3}$ emu/cm^3 in both sections. Specimens from site ISNA only, showed notably higher intensities of induced magnetization. Q-values ranged between 0.9 and 3.5 in specimens from the road section and between 2.6 and 4.4 in the Jhumka Nala specimens (Table II).

Alternating fields

From each site at least one pilot specimen was progressively demagnetized in 16—20 steps up to peak values between 700 and 1500 Oe (Fig. 5A, 5C, 5E, 5G, 5I, 5K). In most specimens a slight northwards and downwards directed present local field component (Fig. 4D), probably of viscous character, could be eliminated at peak values below 100 Oe (sites ISOA—ISOD, Fig. 5K) or below 200 Oe peak value (sites ISNA—ISNI, Fig. 5A, 5G). The remaining intensity of magnetization was more than 95% for the specimens of sites ISOA—ISOD and more than 85% for the specimens of sites ISNA—ISNI (Fig. 6A). Upon continued AF-treatment from peak values of 100—200 Oe onwards up to ultimate peak values of 700—1500 Oe, the vectorgraphs reveal a straight line towards the origin (Fig. 5A, 5C, 5E, 5G, 5I, 5K). This indicates that only one single component becomes gradually removed. For a determination of the mean direction of this characteristic component, at least five more specimens from each site were subjected to partial progressive AF-demagnetization in five steps from 250 to 700 Oe peak value. The specimen directions of the characteristic component group well in the NW-quadrant, pointing upwards (Fig. 2B, 3B, 4B). However, the characteristic component in specimens from some sites (i.e. all specimens from site ISNH, part of the specimens from sites ISNI and ISNA and an occasional specimen from sites ISNE and ISNF) reveals aberrant low inclination directions, streaking towards the present local field direction (Fig. 4B, 5C, 5E). This phenomenon occurs only in the specimens of some sites on the slightly weathered road section. Therefore, we attribute this phenomenon to a simultaneous decay upon AF-treatment of the primary magnetization component

TABLE II

Measurement results from the Sonhat sill dolerite

A. Initial NRM results

Site	Sample*[1]	Site-mean dir. (degrees)		a_{95} (deg)	k	N*[2]	Intensity*[3]	Induced*[3]	Q-value
ISNA	8(14)	350	−3.5	10.5	33	7	46—91	43—52	0.9—1.9
ISNB	8(16)	343	−12	7.5	66	7	13—22	8—14	1.2—2.2
ISNC	8(12)	343.5	−15	7	80.5	7	17—32	10—13	1.6—2.7
ISND	8(15)	346.5	−22.5	4	264.5	7	18—23	11—13	1.6—2.0
ISNE	8(14)	347.5	−14	8	50.5	8	20—24	9—11	2.1—2.5
ISNF	8(16)	349	−10	5.5	117.5	7	22—27	12—14	1.8—2.3
ISNG	8(13)	348.5	−13.5	4	208	7	24—27	12—14	1.8—2.2
ISNH	8(16)	356.5	+15.5	3.5	283.5	7	16—64	6—19	2.4—3.4
ISNI	8(11)	346.5	+7.5	6	96.5	8	13—29	10—12	1.3—2.6
ISOA	9(17)	348.5	−23	2.5	493.5	7	29—32	10—11	2.6—3.1
ISOB	8(11)	333	−18	4	207.5	8	45—52	11—13	3.7—4.3
ISOC	8(16)	341.5	−27.5	5	165	6	34—47	12—14	2.8—3.8
ISOD	7(14)	341.5	−25.5	5.5	122.5	7	31—35	11—12	2.8—3.3

B. Results after AF-treatment

Site	Sample	Site-mean dir. (degrees)		a_{95} (deg)	k
ISNA	5	343	−19	13.5	34
ISNB	6	344	−31.5	4	257
ISNC	6	341	−34.5	3	539
ISND	6	342.5	−36.5	3	504
ISNE	5	348	−32	3.5	417.5
ISNF	5	347	−31	3.5	554.5
ISNG	6	339	−28.5	5	174
ISNH	6	353	+7	4	253.5
ISNI	6	331.5	−20.5	32	5.5
ISOA	6	336	−32.5	3.5	362.5
ISOB	5	333.5	−29.5	2.5	1152
ISOC	6	333	−31	2.5	692.5
ISOD	6	335.5	−33.5	4	309.5
Mean	10*[4]	340	−32	3.2	235

C. Results after thermal treatment

Site	Sample	Site-mean dir. (degrees)		a_{95} (deg)	k
ISNA	2	331	−38.5	—	—
ISNB	2	336	−41.5	—	—
ISNC	1	340	−32	—	—
ISND	7	343	−33	4.5	174.5
ISNE	5	343.5	−30	7	118
ISNF	6	336.5	−31.5	9	58.5
ISNG	7	336.5	−32	4	238
ISNH	7	345	−14	7.5	66.5
ISNI	6	337.5	−17.5	9.5	52.5
ISOA	6	336	−30	2	909.5
ISOB	4	330.5	−31	4	564
ISOC	5	335	−33	3	603.5
ISOD	6	334	−32.5	4	254
Mean	8*[5]	337	−31.5	2.7	434

D. Alternating fields and thermal results combined per site

Sites	Mean-site dir.		a_{95}	k	After dip correction		Pole position	Corresponding dir. at Nagpur	
11*[6]	338.6°	−32.3°	2.3°	394.5	340.1°	−44.1°*[7]	37°S 105°E	337°	−45.5°

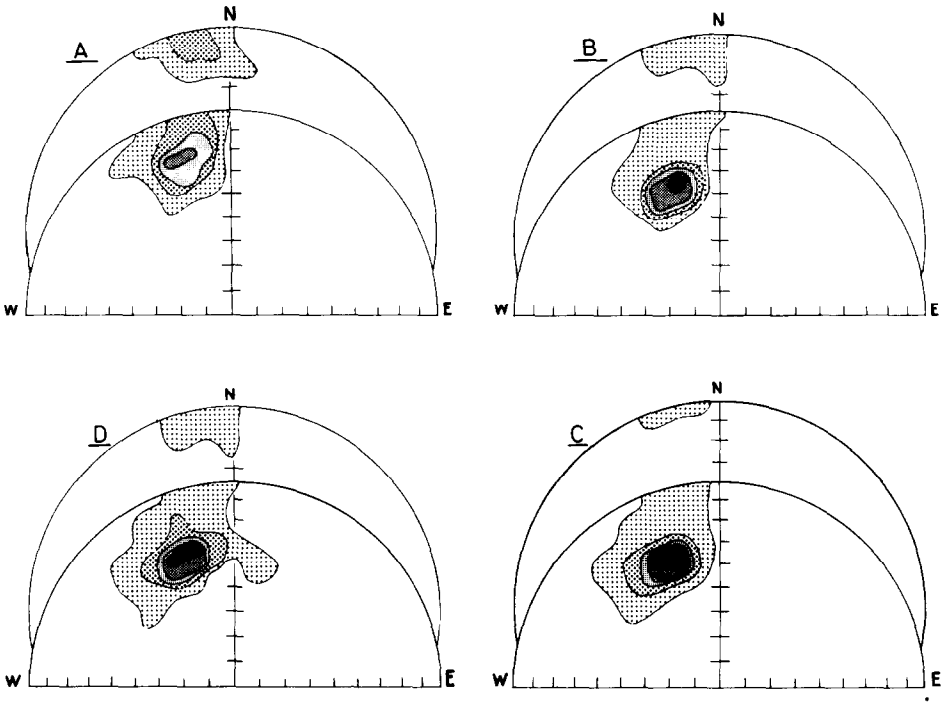

Fig. 2. Density distribution of remanent magnetization directions in equal-area projection. Only the northern quadrants of the upper and lower hemisphere are shown. The partly visible quadrants show directions pointing downwards, the completely visible quadrants show directions pointing upwards.
A. Initial directions. B. AF-treated directions. C. Thermally treated directions. D. Combined AF- and thermal-treated directions.
A streaking towards the present local field direction, dipping about 30 degrees downwards, is clearly visible in the initial directions (A). To a lesser extent the same streaking remains visible after AF- and/or thermal treatment (B, C and D). This is due to incomplete elimination of secondary components in some sites (especially sites ISNH and ISNI). Results from these sites were excluded from the computation of the mean-site direction.

---

*1 Between brackets, number of specimens.
*2 N = number of specimens chosen for AF- and/or thermal treatment.
*3 Intensity = intensity of NRM in units of 10^{-4} emu/cm^3.
Induced = intensity of induced magnetization in units of 10^{-4} emu/cm^3 (H = 0.44 Oe).
*4 Results from sites ISNA, ISNH and ISNI are excluded.
*5 Results from sites ISNA, ISNB, ISNC, ISNH, ISNI are excluded.
*6 Results from sites ISNH, ISNI are excluded.
*7 The direction of the Upper Deccan Traps from the Western Ghats, extrapolated to the Sonhat area according to the central axial dipole field formulae is: D = 343°, I = −42.5°.

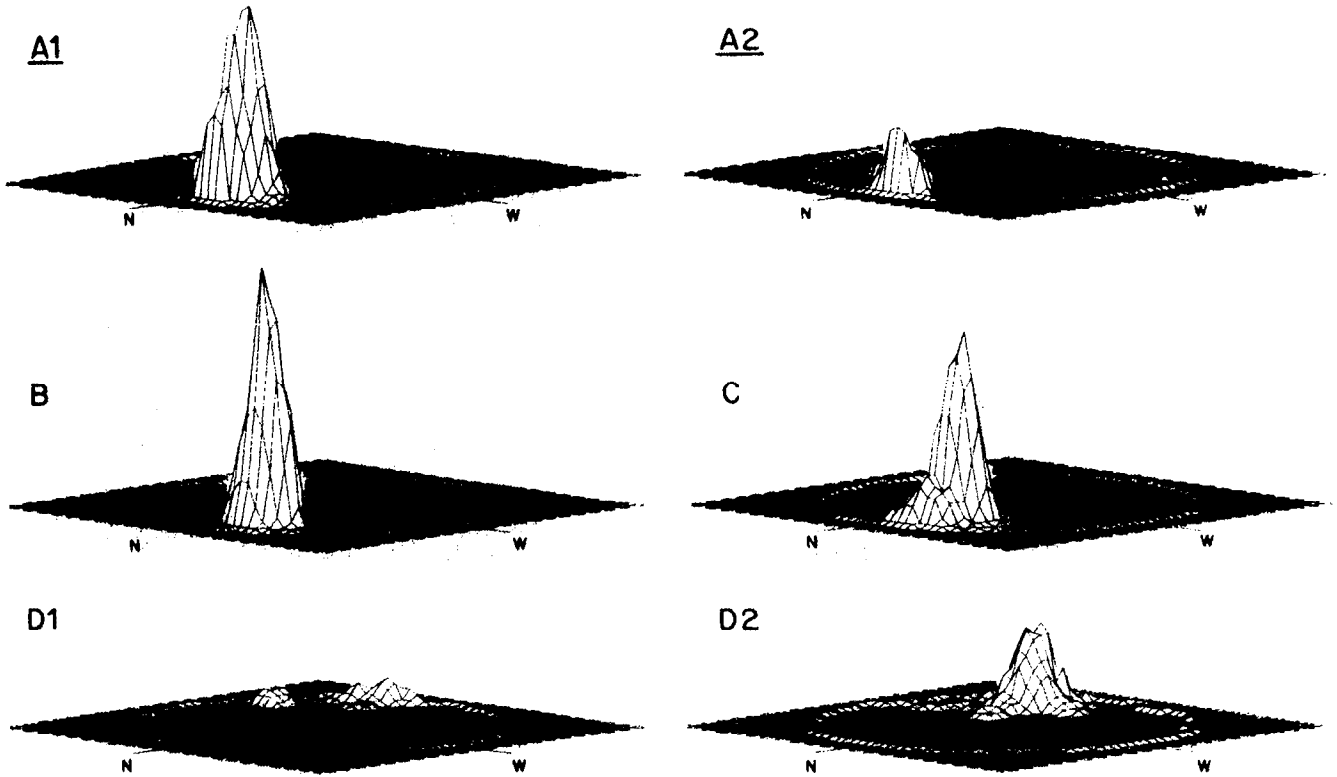

Fig. 3. Density distribution of remanent magnetization directions, represented as a three-dimensional perspective view of an equal-area projection. The view is taken from the northwest. The rim on the figures represents the outline of the equal-area projection.

A1. Initial specimen directions, upper hemisphere. A2. Idem, lower hemisphere. B. AF-treated specimen directions, upper hemisphere only. C. Thermally treated specimen directions, upper hemisphere only.

Upon thermal treatment, the specimens show a peculiar self-reversal tendency. The resulting opposite magnetization directions are shown in Fig. D1 (upper hemisphere only) and Fig. D2 (lower hemisphere only).

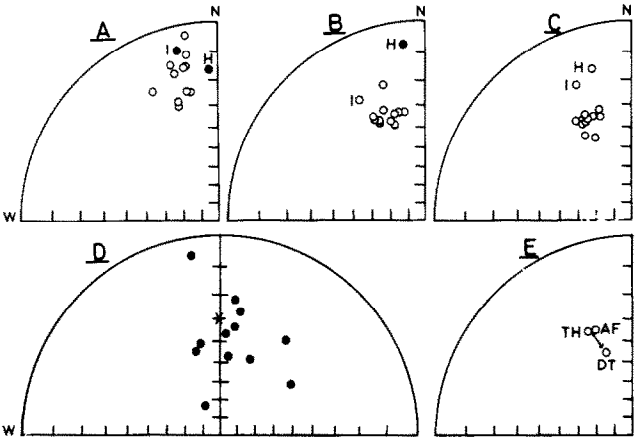

Fig. 4. Stereographic projection of site-mean directions (A, B, C). The circles denote directions pointing upwards and the dots denote directions pointing downwards. Note the aberrant site-mean directions from sites ISNH and ISNI.
A. Initial site-mean directions. B. Site-mean directions, resulting after AF-treatment. C. Idem, after thermal treatment. D. Present local field directions, eliminated in some specimens by AF- or thermal treatment. The asterisk denotes the present local field direction at the sampling locality, dipping downwards. E. Mean-site directions, resulting after alternating-field (AF) or thermal (TH) treatment.
DT represents the mean Upper Deccan Trap direction (normal polarity) at the present sampling area, computed according to the central axial dipole field formulae.

and another hard magnetization component probably resulting from a partly limonitisation of the ore-minerals in these sites. These aberrant site results are excluded from the statistical computation. The results from the remaining sites give a mean-site direction: $D = 340°$, $I = -32°$ ($k = 235$, $a_{95} = 3°$, $N = 10$; Table II), which direction is considered to represent the primary magnetization component.

The rejected apparent "pseudo" stable low-inclination directions are misleading because the demagnetization graphs might be interpreted in the sense that only one "single" component has remained (Fig. 5C, 5E). This "single" component could erroneously be interpreted to represent the primary magnetization.

It must be emphasized here that a probable explanation for these aberrant directions in terms of an orientation error can be ruled out. Neither can these aberrant directions be attributed to the well-known occurrence of "oblique direction," because no signs of a field reversal were found.

In order to obtain a better separation between the primary component and any existing low-temperature oxidation component in the case of these "pseudo" stable low-inclination directions, we subjected the already AF-treated specimens, or in some cases the other specimens from the same sample, to progressive thermal cleaning as well.

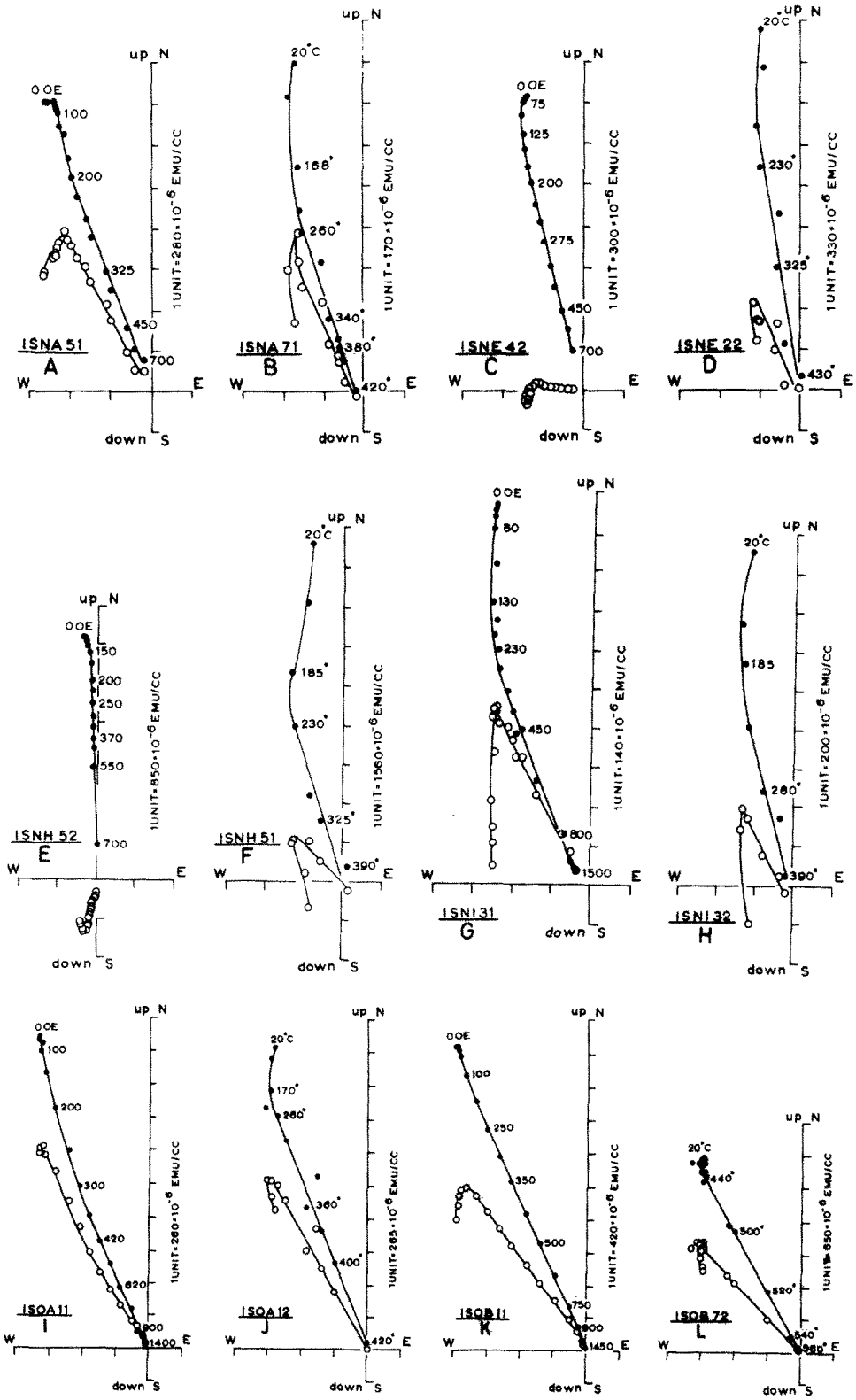
ISNA 51
A
1UNIT=280×10⁻⁶ EMU/CC
ISNA 71
B
1UNIT=170×10⁻⁶ EMU/CC
ISNE 42
C
1UNIT=300×10⁻⁶ EMU/CC
ISNE 22
D
1UNIT=330×10⁻⁶ EMU/CC
ISNH 52
E
1UNIT=850×10⁻⁶ EMU/CC
ISNH 51
F
1UNIT=1560×10⁻⁶ EMU/CC
ISNI 31
G
1UNIT=140×10⁻⁶ EMU/CC
ISNI 32
H
1UNIT=200×10⁻⁶ EMU/CC
ISOA 11
I
1UNIT=260×10⁻⁶ EMU/CC
ISOA 12
J
1UNIT=265×10⁻⁶ EMU/CC
ISOB 11
K
1UNIT=420×10⁻⁶ EMU/CC
ISOB 72
L
1UNIT=850×10⁻⁶ EMU/CC
up N
down S
W
E
0 OE
20°C

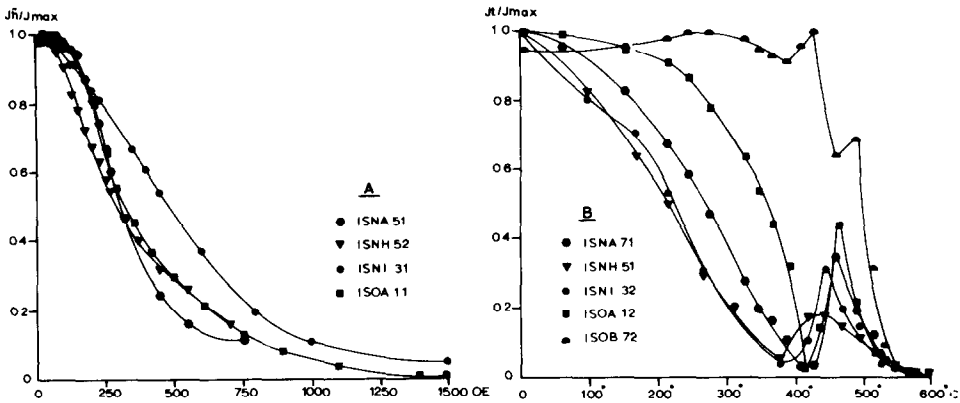

Fig. 6. Normalized intensity decay curves of total remanent magnetization during treatment in alternating fields (A) or by thermal methods (B). The peculiar hump shape of the thermal decay curves — between 400 and 600°C — is due to the self-reversal tendency of the magnetization.

Thermal cleaning

At least one specimen from each site was subjected to a progressive thermal cleaning in about twenty steps up to peak temperatures of 600° C. From the remaining specimens at least five from each site were chosen for partial progressive treatment in about eleven steps in the temperature interval between 260 and 600° C.

After the later heating/cooling cycles (in magnetic field-free space) up to temperatures above 400° C, it was found that the specimens quickly acquired a large viscous magnetization component when placed at room temperature in the earth's field. This hampered the measurements to a large extent. Therefore, special care was taken to eliminate influences of the ambient field on the specimens as much as possible during the measuring procedure.

The results from the thermal treatment are comparable to those from the AF-treatment; a present local field component of slight intensity and probably of viscous character was eliminated at temperatures around 200° C

Fig. 5. Demagnetization diagrams of specimens cleaned in alternating fields (A, C, E, G, I, K) or by thermal methods (B, D, F, H, J, L). The points represent successive positions — in orthogonal projection — of the end of the resultant magnetization vector during the progressive demagnetization. Circles denote projections on the vertical east—west plane. Dots denote projections on the horizontal plane. Numbers denote successive oersted peak values of the applied alternating fields or successive peak values of the applied temperatures. Compare the alternating-field and the thermal results from both specimens (in some cases specimens from the same sample) from the same site.

(Fig. 4D, 5B, 5D, 5F, 5H, 5J, 5L). From these temperatures onwards, the straight course of the vectorgraphs gives the impression that only one single component was gradually removed. The thermal decay curves in general reveal Curie temperatures around 400° C (Fig. 6B). In accordance with the ore-microscopy results, these temperatures point to a titanomagnetite as the main magnetization carrier. The direction of the characteristic component, which is in most sites similar to the direction of the characteristic AF-component (Fig. 2C, 3C, 4C), was determined in all specimens by means of a least-square approximation procedure (Table II). The results of the thermal treatment compared with those from the AF-treatment point to a better separation between the characteristic component and the previously mentioned hard magnetization component. This holds for specimens from site ISNH in particular and to a lesser extent in the other previously mentioned aberrant specimens (Fig. 4B, 4C, 5C, 5D, 5E, 5F), resulting (see Table II) in higher inclinations (ISNH) or better grouping directions (ISNI). The secondary hard magnetization component probably results from a partly limonitisation of the ore-minerals after recent denudation of the rocks. In spite of the improved separation between both components in sites ISNH and ISNI, the elimination of the hard secondary component does not appear to be complete, because the thermally obtained site-mean directions from sites ISNH and ISNI seem still somewhat biased towards the present local field direction. Therefore, these sites (ISNH and ISNI) are excluded from a computation of the mean-site direction. The thermal results from sites ISNA, ISNB and ISNC are excluded as well because of a too small amount of specimen data (Table II).

The resulting mean-site direction is: $D = 337°$, $I = -32°$ ($k = 434$, $a_{95} = 2.7°$, $N = 8$). This direction is coincident with the mean-site direction resulting from AF-treatment (Fig. 4E).

A PARTIAL SELF-REVERSAL

Several special features of the thermal demagnetization results can be interpreted in terms of a partial self-reversal of the magnetization. These features are: the second peak in the decay curves (Fig. 6B) and the reversed directions in the demagnetization graphs (Fig. 7, 8, 9, 3D1, 3D2). Research on this self-reversal is in progress now and detailed results will be dealt with in a separate paper (Dankers and Klootwijk, in preparation).

Preliminary measurements confirm the reality of this partial self-reversal. Some specimens were heated stepwise to higher temperatures in a rotating-sample furnace (Weijts et al., 1967) in argon atmosphere and placed in a field-free space. Between two successive steps the specimens were cooled down to room temperature. The intensity of remanent magnetization was measured continuously during all heating/cooling cycles. The successive intensity changes are shown for one specimen in Fig. 10. In the case of this specimen ISOA92, during two cycles after heating up to about 500° C, the

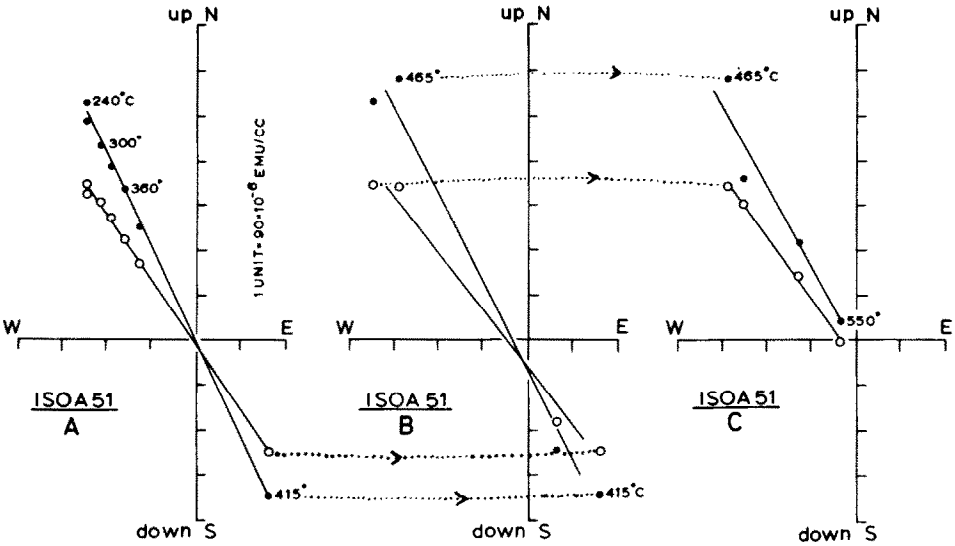

Fig. 7. Demagnetization diagrams of specimen ISOA51, showing opposite directions upon thermal treatment, due to the self-reversal tendency. For reasons of visibility the demagnetization graph is represented as a tripartite diagram (A: 240—415°C; B: 415—465°C; C: 465—550°C). Note the neatly opposite magnetization directions.

intensity changed sign and reached negative values at room temperature. In general this phenomenon occurred after heating up to temperatures between 400 and 500°C (Fig. 6, 7, 8, 9). This phenomenon accords to the reversed directions found in the demagnetization graphs, which were measured after

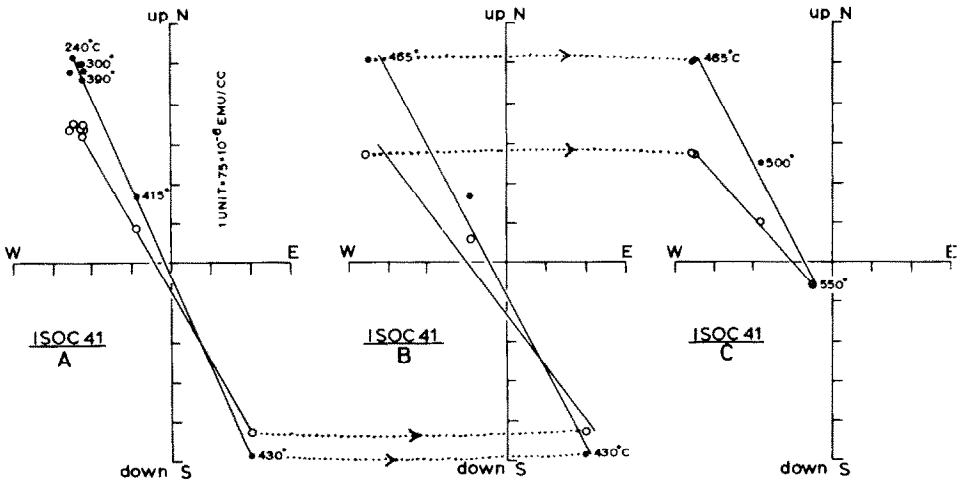

Fig. 8. Threefold demagnetization diagram of specimen ISOC41 upon thermal treatment. For explanation see caption to Fig. 7.

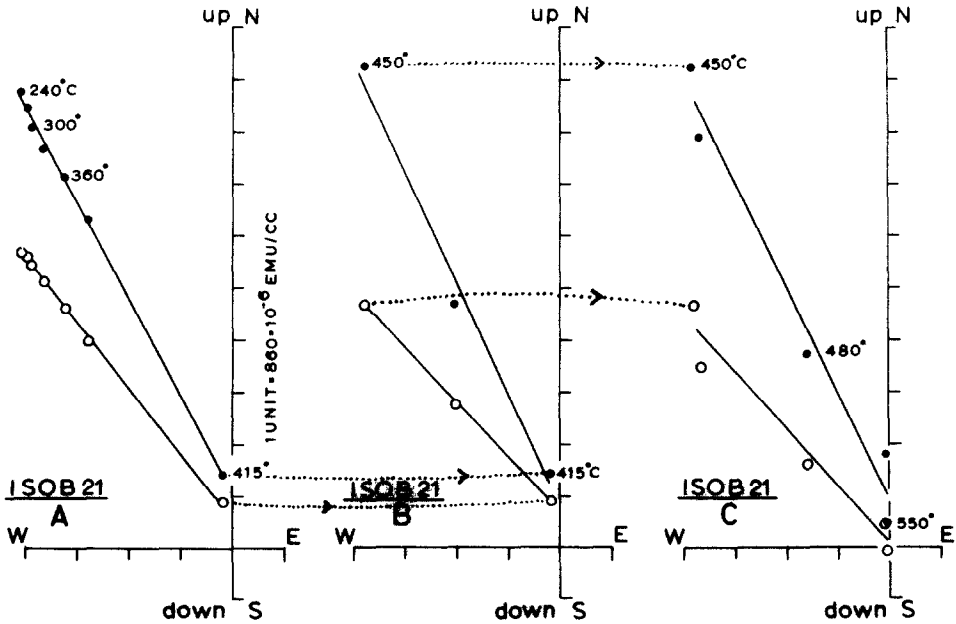

Fig. 9. Threefold demagnetization diagram of specimen ISOB21, which reveals the same self-reversal tendency as demonstrated in Fig. 7 and 8. However, in this case the tendency is less pronounced and the successive measurement results remain on the same site of the origin.

cooling down to room temperature (Fig. 7, 8, 9, 3D1, 3D2). A possible explanation for these preliminary results might be essentially similar to the explanation given by Creer et al. (1970) for a partial self-reversal observed in the titanomagnetites of samples from the Rauher Kulm basalt (Germany). The peculiar hump-shaped intensity curves might be explained by a negative coupling of two different magnetic phases. Upon successive heating a new daughter phase is formed, presumably due to solid-state exsolution reactions. The superparamagnetic part of this daughter phase might cause the strong viscous magnetization which is noted during subsequent measurement on the astatic magnetometer after thermal treatment up to temperatures above 400° C. During progressive heating, in zero field, this daughter phase grows through the superparamagnetic stage and acquires an opposite magnetization due to negative interaction with the not yet completely eliminated magnetization of the mother phase. Upon further heat treatment, the subsequent elimination of the magnetization of the mother phase and the prolonged changes in the daughter phase probably by their mutual interaction result into the peculiar reversed directions at room temperature (Fig. 7, 8, 9, 10, 3D1, 3D2).

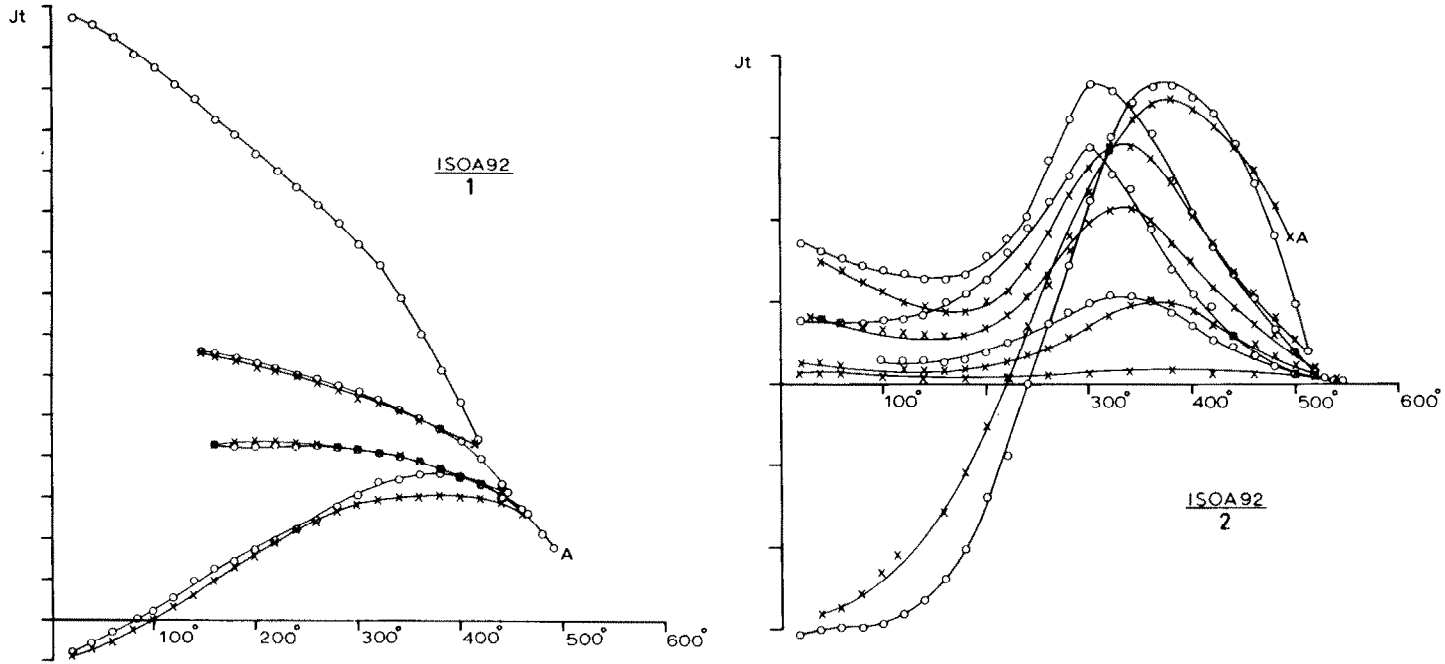

Fig. 10. Successive curves revealing the particular changes in intensity of magnetization upon thermal treatment of specimen ISOA92. The specimen is heated to a certain temperature (heating curve denoted by circles) and is subsequently cooled down to about room temperature (cooling curve, denoted by crosses). During each successive heating/cooling cycle (eight cycles in all) subsequently higher temperatures are reached. In both figures the intensity is given in arbitrary units. Fig. 10-2 is an enlarged version of Fig. 10-1. For reason of visibility the vertical scaling is two times enlarged in Fig. 10-2. Point *A* in Fig. 10-1 depicts the endpoint of the heating trajectory in the fourth heating/cooling cycle. This point *A* (10-1) corresponds with point *A* in Fig. 10-2, depicting here the starting point of the cooling trajectory in the fourth heating/cooling cycle. Note that the intensity changed its sign during the cooling trajectories of the third (10-1) and the fourth cycle (10-2) and during the heating trajectories of the fourth (10-1) and the fifth (10-2) cycle. The end points of the cooling trajectory (i.e. the points nearest to the coordinate axis) correspond to similar measuring results obtained during progressive thermal demagnetizations as represented in Fig. 7, 8, 9 and 3D1, 3D2. These sign changes of the magnetization intensity cause the successive opposite directions in the threefold demagnetization graphs (Fig. 7, 8, 9). In some instances after a heating/cooling cycle the specimen (ISOA92) was taken out of the furnace and the magnetic field-free space for directional measurements. Subsequent acquisition of viscous magnetization caused the discontinuities, visible between the graphs of the successive heating/cooling cycles.

INTERPRETATION OF DIRECTIONAL RESULTS

The characteristic directions computed from alternating field- and thermal treatment (Table II) agree very well with each other (Fig. 4E). Therefore, the AF- and thermal results are combined per site. The ultimate mean-site direction is: $D = 338.5°$, $I = -32°$ ($k = 395$, $a_{95} = 2.3°$, $N = 11$; sites ISNH and ISNI are excluded).

A K/Ar dating for this sill has been made by E.H. Hebeda in the Z.W.O. Laboratory for Isotope Geology (Amsterdam). This dating revealed an age of 60.0 ± 3.0 m.y. (Table III). Wellmann and McElhinny (1970) obtained K/Ar datings for the Deccan Traps ranging between 59 and 64 m.y. These ages are supported by K/Ar studies by Kaneoka and Haramura (1973). This proves the normal magnetized Sonhat sill to be contemporaneous with the Upper Deccan Trap flows, because these flows show magnetizations of normal polarity as well. However, the mean palaeomagnetic direction of the Sonhat sill deviates from the direction of the Upper Deccan Trap flows (Fig. 4E), extrapolated to the Sonhat area according to the central axial dipole field formulae ($D = 343°$, $I = -42.5°$ according to data by Wensink and Klootwijk (1971) from the Western Ghats; or $D = 347.5°$, $I = -46°$ according to a recent compilation of data from Upper Deccan flows of normal polarity by Closs et al. (in preparation)). After application of a correction for the local dip of the strata in which the sill is intruded, both directions become coincident (Fig. 4E). Therefore, it can safely be assumed that the Gondwana strata in the Sonhat basin acquired their northward dip *after* intrusion of this sill. This conclusion is important for the interpretation of the local geological situation (P.K. Ghosh and D. Mukherjee, personal communication, 1969). The palaeolatitude pattern according to this Sonhat sill pole (dip correction applied) is shown in Fig. 11.

From the present results it must be concluded that Athavale and Verma's (1970) palaeomagnetic arguments in support of a continuous magmatic activity, passing from Rajmahal Trap times (100—105 m.y., McDougall and McElhinny, 1970) up to Deccan Trap times (60—65 m.y., Wellmann and

TABLE III

Potassium—argon age of the Sonhat sill*

Sample No.	K (Wt %)	Rad. ^{40}Ar (ppm. Wt)	Atmospheric ^{40}Ar (% total ^{40}Ar)	Age** (m.y.)
70 IND 3	0.446	$1.89 \cdot 10^{-3}$	42.2	60.0 ± 3.0
	0.446	$1.95 \cdot 10^{-3}$	33.9	

* After E.H. Hebeda, personal communication, 1973.

** Calculated with ^{40}K constants: $\lambda_e = 5.85 \cdot 10^{-11}$/year; $\lambda_\beta = 4.72 \cdot 10^{-10}$/year; $^{40}K/K = 0.0118$ at %.

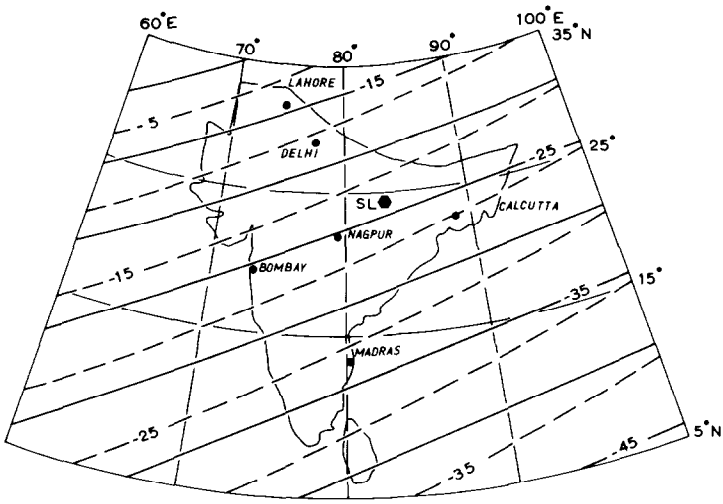

Fig. 11. Palaeolatitude map (full line) for the Indian subcontinent as deduced from the Sonhat sill palaeomagnetic data. The proposed full-line pattern is obtained after application of a dip correction. For comparison a virtual pattern is demonstrated which would be obtained if one refrained from applying this dip correction. Both patterns are computed according to the central axial dipole field formulae.

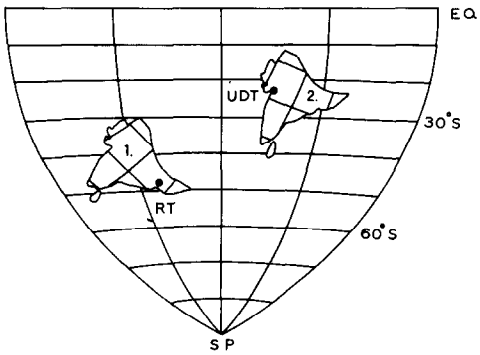

Fig. 12. Comparison of orientation and position of the Indian subcontinent (in Aitoff projection), according to palaeomagnetic data from the Rajmahal Traps (*1*) and the Upper Deccan Traps (*2*). The longitudinal positions of the subcontinent are arbitrary. *RT* denotes the eruption area during the Rajmahal Trap extrusion (100—105 m.y.). *UDT* denotes the probable eruption area in the later phase of the Deccan Trap extrusion (60—65 m.y.). Note that the eruption area of the Rajmahal Traps was located much further to the south than the probably eruption area of the Upper Deccan Traps at the time of the respective extrusions.

McElhinny, 1970; Kaneoka and Haramura, 1973) are ambiguous. Their palaeomagnetic results, for which no radiometric age control has been obtained, show directions which are irregularly spread between the Rajmahal Trap direction (Klootwijk, 1971) and the Deccan Trap direction (Wensink and Klootwijk, 1971; Wensink, 1973). Athavale and Verma's results have been obtained after AF-treatment, generally up to 100 Oe only, whereas the possible application of a dip correction has not been taken into consideration. However, from the present results one should be aware that a more elaborate cleaning might be necessary, and that post-intrusional disturbances of the strata seem to have occurred. Therefore, the theory of a single continuous magmatic activity (Pascoe, 1959, 1963, Krishnan, 1968) passing from the Rajmahal Trap eruption phase in eastern India, through a hypabyssal phase of dolerite dyke and sill intrusions in the intervening tract of Gondwana basins, to the Deccan Trap eruption phase in western India, seems not to be backed in an unambiguous way by Athavale and Verma's data.

Apart from the probability of such a prolonged continuous activity, passing over a period of about 40 m.y. without signs of compositional changes, it must be emphasized that the hypothesis of continuous magmatic activity does not agree with the recently discussed Plume Theory (Morgan, 1971, 1972; Grommé and Vine, 1972; McElhinny, 1973). If one leaves out of question a possible polar wandering, the hypothesis of a mantle fixed hot spot would imply a meridional movement of the Indian subcontinent in a direction from north to south. However, the actual movement was in the opposite direction (Fig. 12), as can be deduced from the palaeomagnetic data concerned (Klootwijk, 1971; Wensink and Klootwijk, 1971; Wensink, 1973).

ACKNOWLEDGEMENTS

Thanks are due to Dr. J.D.A. Zijderveld and Prof. J. Veldkamp for their stimulating interest and for critically reading the manuscript.

Ir. G.A.E.M. Hermans and Dr. C. Maijer, kindly studied the opaque minerals.

I gratefully acknowledge the radiometric dating by Dr. E.H. Hebeda.

This study was supported by the Netherlands Organisation for the Advancement of Pure Research (Z.W.O.).

REFERENCES

Athavale, R.N. and Verma, R.K., 1970. Palaeomagnetic results on Gondwana dykes from the Damodar Valley coal fields and their bearing on the sequence of Mesozoic igneous activity in India. Geophys. J., 20: 303–316.

Closs, H., Narain, H., Klootwijk, C.T. and Garde, S.C., in preparation. Continental margins of India, including a palaeomagnetic analysis. Submitted to the Penrose Conference Proceedings on the Geology of Continental Margins.

Creer, K.M., Petersen, N. and Petterbridge, J., 1970. Partial self-reversal of remanent magnetization and anisotropy of viscous magnetization in basalts. Geophys. J., 21: 471—483.

Fermor, L.C., 1914. On the geology and coal resources of Korea State, Central Provinces. Mem. Geol. Surv. India, 16 (2): 148—245.

Fox, C.S., 1934. The Lower Gondwana coalfields in India. Mem. Geol. Surv. India, 59: 386 pp.

Grommé, S. and Vine, F.J., 1972. Palaeomagnetism of the Midway atoll lavas and northward movement of the Pacific plate. Earth Planet. Sci. Lett., 17: 159—168.

Kaneoka, I. and Haramura, H., 1973. K/Ar ages of successive lava flows from the Deccan Traps, India. Earth Planet. Sci. Lett., 18: 229—236.

Klootwijk, C.T., 1971. Palaeomagnetism of the — Upper Gondwana — Rajmahal Traps, Northeast India. Tectonophysics, 12: 449—467.

Krishnan, M.S., 1968. Geology of India and Burma, Higginbothams, Madras, 536 pp.

McDougall, I. and McElhinny, M.W., 1970. The Rajmahal Traps of India. K/Ar ages and palaeomagnetism. Earth Planet. Sci. Lett. 9: 371—378.

McElhinny, M.W., 1973. Mantle plumes, palaeomagnetism and polar wandering. Nature, 241: 523—524.

Morgan, W.J., 1971. Convection plumes in the lower mantle. Nature, 230: 42—43.

Morgan, W.J., 1972. Deep mantle convection plumes and plate motions. Bull. Am. Assoc. Pet. Geol., 56: 203—213.

Pascoe, E.H., 1959. A Manual of the Geology of India and Burma, 2. Government Press, Delhi, pp. 485—1343.

Pascoe, E.H., 1963. A Manual of the Geology of India and Burma, 3. Government Press, Delhi, pp. 1345—2129.

Wadia, D.N., 1953. Geology of India. Macmillan, London, 531 pp.

Weijts, A.G.L.M., Poulis, J.A. and Spence, R.D., 1967. The use of a commercial available fluxgate magnetometer in the determination of the Curie point of rock samples. In: D.W. Collinson, K.M. Creer and S.K. Runcorn (Editors), Methods in Palaeomagnetism. Elsevier, Amsterdam, pp. 447—449.

Wellmann, P. and McElhinny, M.W., 1970. K/Ar age of the Deccan Traps, India. Nature, 227: 595—596.

Wensink, H., 1973. Newer palaeomagnetic results of the Deccan Traps, India. Tectonophysics, 17: 41—59.

Wensink, H. and Klootwijk, C.T., 1971. Palaeomagnetism of the Deccan Traps in the Western Ghats near Poona (India). Tectonophysics, 11: 175—190.